Neurobiology of Aging 34 (2013) 1700–1707

Contents lists available at SciVerse ScienceDirect

Neurobiology of Aging

journal homepage: www.elsevier.com/locate/neuaging

Brain structure in asymptomatic *FMR1* premutation carriers at risk for fragile X-associated tremor/ataxia syndrome

Giovanni Battistella [a,1], Julien Niederhauser [b,1], Eleonora Fornari [a,c], Loyse Hippolyte [d], Aline Gronchi Perrin [b], Gaetan Lesca [e], Francesca Forzano [f], Patric Hagmann [a], Francois J.G. Vingerhoets [b], Bogdan Draganski [g,h,i], Philippe Maeder [a,2], Sébastien Jacquemont [d,2,*]

[a] *Department of Radiology, Centre Hospitalier Universitaire Vaudois and University of Lausanne, Lausanne, Switzerland*
[b] *Service of Neurology, Department of Clinical Neurosciences, Centre Hospitalier Universitaire Vaudois, Lausanne, Switzerland*
[c] *Centre d'Imagerie Biomédicale, Centre Hospitalier Universitaire Vaudois, Lausanne, Switzerland*
[d] *Service of Medical Genetics, Centre Hospitalier Universitaire Vaudois, Lausanne, Switzerland*
[e] *Service de génétique moléculaire et clinique, hôpital Edouard-Herriot et service de génétique, hôpital Femme-Mère-Enfant, Lyon, France*
[f] *Division of Medical Genetics, Galliera Hospital, Genova, Italy*
[g] *LREN-Departement des neurosciences cliniques, Centre Hospitalier Universitaire Vaudois, University of Lausanne, Lausanne, Switzerland*
[h] *Max-Planck Institute for Human Cognitive and Brain Sciences, Leipzig, Germany*
[i] *Mind and Brain Institute, Charité Berlin, Berlin, Germany*

ARTICLE INFO

Article history:
Received 13 November 2012
Accepted 3 December 2012
Available online 5 January 2013

Keywords:
FXTAS
Premutation
Genetics
Volumetric MRI
DTI

ABSTRACT

Fragile X-associated tremor/ataxia syndrome (FXTAS), a late-onset movement disorder affecting *FMR1* premutation carriers, is associated with cerebral and cerebellar lesions. The aim of this study was to test whether computational anatomy can detect similar patterns in asymptomatic *FMR1* premutation carriers (mean age 46.7 years) with qualitatively normal -appearing grey and white matter on brain MRI. We used a multimodal imaging protocol to characterize brain anatomy by automated assessment of gray matter volume and white matter properties. Structural changes in the hippocampus and in the cerebellar motor network with decreased gray matter volume in lobule VI and white matter alterations of the corresponding afferent projections through the middle cerebellar peduncles are demonstrated. Diffuse subcortical white matter changes in both hemispheres, without corresponding gray matter alterations, are only identified through age × group interactions. We interpret the hippocampal fimbria and cerebellar changes as early alterations with a possible neurodevelopmental origin. In contrast, progression of the diffuse cerebral hemispheric white matter changes suggests a neurodegenerative process, leading to late-onset lesions, which may mark the imminent onset of FXTAS.

1. Introductions

Fragile X-associated tremor/ataxia syndrome (FXTAS) is an X-linked late-onset neurodegenerative disorder caused by a CGG expansion in the 5′ untranslated region of the *FMR1* gene. The mean age of onset is 62 years and the penetrance is incomplete (Jacquemont et al., 2004; Li and Jin, 2012). Men are more commonly affected and the clinical symptoms include gait ataxia, intention tremor, parkinsonism, and peripheral neuropathy. Patients also present with cognitive decline and psychiatric symptoms (Bourgeois et al., 2011; Jacquemont et al., 2003; Sevin et al., 2009).

Neuropathologic studies (Greco et al., 2002; Greco et al., 2006) in advanced cases of FXTAS have shown white matter abnormalities ranging from microscopic pallor to severe degeneration, primarily in the subcortical white matter, with involvement of arcuate fibers and sparing of periventricular white matter. The areas involved showed varying degrees of spongiosis with both myelin and axonal loss, but determining the relative contribution of these 2 alterations to the pathophysiology of FXTAS has not yet been possible. The knock-in mouse model has not helped to clarify the pathophysiology because it does not display white matter lesions (Brouwer et al., 2008).

Although the most characteristic neuroimaging features of FXTAS are T2 hyperintensities in the middle cerebellar peduncles (MCP), nonspecific diffuse white matter lesions are also present throughout the cerebral hemispheres and cerebellum (Brunberg

* Corresponding author at: Service de génétique, Centre Hospitalier Universitaire Vaudois, 1011 Lausanne, Switzerland. Tel.: +41 21 314 55 93; fax: +41 (0)21 314 33 92.
E-mail address: sebastien.jacquemont@chuv.ch (S. Jacquemont).
[1] Shared first authorship.
[2] Shared last authorship.

0197-4580/$ – see front matter © 2013 Elsevier Inc. All rights reserved.
http://dx.doi.org/10.1016/j.neurobiolaging.2012.12.001

et al., 2002). Little is currently known about the physiopathology of these alterations. Anatomic studies based on T1-weighted imaging data failed to detect gray matter changes in asymptomatic carriers when using conservative statistical thresholds. The same study reported conflicting findings in the cerebellum after reducing the search volume to an a priori defined region of interest (Hashimoto et al., 2011a). Two studies reported negative results of a whole-brain assessment of white matter in asymptomatic carriers (Hashimoto et al., 2011b; Wang et al., 2012) and 2 tract of interest (TOI) analyses report conflicting findings in the MCP of older asymptomatic carriers close to the mean onset of FXTAS (58 years of age). Age-related changes in the extreme capsule was the only alteration detected in young asymptomatic carriers (Wang et al., 2012).

Most brain lesions in patients with FXTAS are likely neurodegenerative in nature, but some may be related to a neurodevelopmental process. Several studies in mice suggest that *FMR1* premutation affects CNS functioning during the early stages of development (Chen et al., 2010; Cunningham et al., 2011). Clinical studies have also shown that some cognitive tasks are impaired in premutation carriers without any aging effect (Cornish et al., 2009) and that a series of behavioral symptoms are present in younger premutation carriers (Hessl et al., 2005).

In this study, we adopt a multimodal strategy acquiring T1- and diffusion-weighted images, and magnetization transfer imaging (MTI) to characterize gray matter volume, white matter integrity, and myelin status. Diffusion imaging is a widely used technique and is a sensitive marker of white matter integrity (axonal loss and demyelination and/or dysmyelination) and structural connectivity (Dumas et al., 2012; Hagmann et al., 2008; Kloppel et al., 2008; Moll et al., 2011). The sensitivity of MTI to detect demyelination and/or dysmyelination, even before volumetric alteration, has been previously demonstrated in neurodegenerative disorders, such as Alzheimer's disease and Parkinson's disease (Anik et al., 2007; Fornari et al., 2012; Giulietti et al., 2012; van Es et al., 2006), as well as in developmental studies (Fornari et al., 2007; Xydis et al., 2006).

The aim of this study was to identify early brain markers in young asymptomatic premutation carriers and to provide insight into the relative contribution of both developmental and neurodegenerative processes related to the *FMR1* premutation. We investigated 27 asymptomatic premutation carriers with normal-appearing gray and white matter and 35 controls. Alterations in the motor network of the cerebellum, including lobule VI (anteriorly and the corresponding afferent projections), were found in the group of carriers. A much later involvement of the hemispheric white matter may signal imminent onset of FXTAS. Some alterations show no acceleration with age and could represent a neurodevelopmental (as opposed to degenerative) effect of the premutation, highlighting that different disease mechanisms may be involved in FXTAS.

2. Methods

The study was approved by the local institutional review board and all participants gave informed consent. All participants were men with a family member with fragile X syndrome. Thirty asymptomatic premutation carriers and 37 intrafamilial controls between 20 and 70 years of age were recruited. *FMR1* allele status and CGG repeat size was confirmed in all participants by DNA testing. Participants were included in the premutation group when $55 \leq$ CGG <200 and in the control group when CGG <55. Exclusion criteria included the presence of symptoms suggestive of possible or probable FXTAS (Jacquemont et al., 2003) and white matter alterations visible on fluid attenuated inversion recovery (FLAIR) images examined by an experienced neuroradiologist blinded to the genetic status of the participant. To control for factors influencing white matter lesions, we measured glycosylated hemoglobin (HbA_{1c}) for diabetes, C-reactive protein for inflammation, and blood pressure. Drug use, smoking habits, and past medical history were also assessed. Three premutation carriers were excluded because of white matter lesions in FLAIR images and 2 controls were excluded because of technical problems during magnetic resonance imaging (MRI). The final dataset comprised 27 premutation carriers and 35 controls.

2.1. Global cognitive status

The global cognitive status was assessed in a blind fashion with the Mattis Dementia Rating Scale (MDRS) (Mattis, 1976), a widely used instrument for screening dementia. The MDRS generates a total score (maximum 144) and 5 subscale scores for the cognitive domains of attention, initiation (verbal and motor), constructive praxis, conceptualization, and memory. Based on a previous study with a population of male carriers of the FMR1 premutation (Sevin et al., 2009), we used a cut-off score of 123 for the total score of the MDRS and a score of 25 for the Mini Mental State Examination (MMSE) to exclude individuals with cognitive dysfunction (Crum et al., 1993).

2.2. Neurologic evaluation

Participants underwent a thorough neurologic evaluation. They were assessed using 3 standardized scales: the Clinical Rating Scale for Tremor (Fahn et al., 1993), the motor section of the Unified Parkinson's Disease Scale (Jacquemont et al., 2004; Stebbins and Goetz, 1998), and the International Cooperative Ataxia Rating Scale (Trouillas et al., 1997). We computed the FXTAS rating scale (Leehey et al., 2008), a composite score based on the 3 standardized scales and the tandem test (a sensitive test for cerebellar gait dysfunction). The neurologic examination was videotaped and rated by a movement disorder specialist.

2.3. MRI

All premutation carriers and control subjects were scanned in a 3-T Siemens Trio scanner (Siemens AG, Erlangen, Germany) using a 32-channel head coil. The protocol included a sagittal T1-weighted gradient-echo sequence (MPRAGE), 160 contiguous slices, 1-mm isotropic voxel, repetition time (TR) 2300 milliseconds, echo time (TE) 2.98 milliseconds, field of view 256 mm as a basis for segmentation. FLAIR contrast images were acquired with a voxel size of $0.9 \times 0.9 \times 2.5$ mm, flip angle 150, TR 9500 milliseconds, TE 84 milliseconds, 32 axial slices.

Diffusion-weighted images were acquired using a spin-echo echo planar imaging sequence (64 gradient directions, b value 1000 seconds/mm^2, voxel size $2 \times 2 \times 2.5$ mm, 52 axial slices, TR 6700 milliseconds, TE 89 milliseconds, field of view 192×192 mm) plus 1 volume without diffusion weighting (b value 0 seconds/mm^2) at the beginning of the sequence as anatomic reference for motion and eddy current correction.

MTI was performed by running a gradient-echo sequence (flip angle 20°, 60 axial slices, voxel size $1.3 \times 1.3 \times 2.5$ mm, TR 1750 milliseconds, TE 10 milliseconds, matrix size 192×192 mm) twice, with and without saturation pulse. A Gaussian magnetization transfer (MT) prepulse with a duration of 7.68 milliseconds and a frequency offset of 1.5 kHz was used.

2.4. Diffusion analysis

Diffusion tensor imaging (DTI) analyses were performed with FSL (http://www.fmrib.ox.ac.uk/fsl/index.html). The preprocessing

of the diffusion dataset (64 gradient directions) involved motion and eddy current correction. In this step, each diffusion-weighted image was registered to the b0 image (no diffusion encoding) using a 12-parameter affine transformation. This transformation accounts for motion between scans and for residual eddy current distortions present in the diffusion-weighted images. The diffusion tensor was then estimated (Mori and Zhang, 2006) and the 3 eigenvalues of the tensor were used to compute the fractional anisotropy (FA), the mean diffusivity (MD) (Habas, 2004), the radial (RD) and axial diffusivity maps for each subject on a voxel-by-voxel basis (Pierpaoli and Basser, 1996). These maps were used as the basis of the quantitative analysis of the DTI data.

2.5. Voxel-based analysis

Data preprocessing was carried out using SPM8 (Wellcome Trust Centre for Neuroimaging: http://www.fil.ion.ucl.ac.uk/spm/) running under Matlab 7.11 (MathWorks Inc, Sherborn, MA, USA). For automated tissue classification in gray matter, white matter, and cerebrospinal fluid, the unified segmentation approach was used (Ashburner and Friston, 2005). Aiming at optimal anatomic precision, we then applied spatial registration to the MNI (Montreal Neurological Institute) space using a diffeomorphic registration algorithm (DARTEL) (Ashburner, 2007) followed by spatial smoothing with a Gaussian kernel of 6 mm full-width-at-half-maximum.

For voxel-based analysis on white matter, we implemented a data processing pipeline on the FA, MD, RD, and axial diffusivity maps using the voxel-based quantification data processing method (Draganski et al., 2011). FA maps were coregistered (Maes et al., 1997) to the white matter segments, followed by application of the same transformation parameters to the MD, RD, axial, and magnetization transfer ratio (MTR) maps. Normalization of these maps to the MNI space was performed using the subject-specific diffeomorphic fields from the DARTEL procedure (resampled voxel size of 1.5 mm isotropic), but without scaling by the Jacobian determinants. To enhance the specificity for the white matter tissue class, we performed a combined weighting and smoothing procedure detailed in the Supplementary material S1.

For voxel-based statistical analysis of regional effects, a multiple linear regression model embedded in the General Linear Model framework of SPM8 was used. Group differences were tested including age and total intracranial volume (TIV, the sum of gray matter, white matter, and volume of cerebrospinal fluid) as regressors to control for the effects of these variables. The model tested is: MRI-measure $= \alpha(\text{group}) + \beta(\text{age}) + \gamma(\text{TIV})$. In the interaction analysis, the CGG repeat length was also added to age and TIV as a covariate: MRI-measure $= \alpha(\text{group}) + \beta(\text{age} \times \text{group}) + \gamma(\text{CGG} \times \text{group}) + \delta(\text{age} \times \text{CGG[mean corrected]} \times \text{group}) + \varepsilon(\text{TIV})$. Each scalar map (FA, MD, RD, and axial diffusivity) was tested independently creating 1 design matrix per map. A binary mask of the tissues of interest (gray matter or white matter) was used to ensure inclusion of the same number of voxels in all analyses. Statistical thresholds were applied at $p < 0.05$ after family-wise error (FWE) correction for multiple comparisons over the whole volume of the gray matter/white matter and $k > 40$ for cluster extent (greater than the minimum voxels expected per cluster). In addition, the regions that are known to be affected in the late stage of the disease that showed $p < 0.005$ uncorrected and $k > 40$ for cluster extent (Friston et al., 1994), and survived small volume correction were considered to be significant.

2.6. MTR

The MTR allows the evaluation of the MT exchange between 2 sets of images, the one acquired without saturation pulse (M0) and the other one with saturation pulse (Anik et al., 2007). Dousset et al. (1992) were the first to use MTI clinically to characterize tissue. They defined MTR as:

$$\text{MTR} = \frac{M_o - M_s}{M_o} \times 100$$

MTR images were available just for a subsample of our population (23 controls and 17 carriers). Information derived from these maps was used to improve the biological interpretation of the results of the voxel-based analysis on the diffusion data. To this end, the mean MTR value in the clusters showing an alteration in the MD and in the RD was calculated for each subject and compared between the 2 cohorts using a nonparametric test.

3. Results

The premutation carriers and controls do not differ in age, educational level, and potential confounding factors such as diabetes, hypertension, smoking habits, and drug consumption. Global cognitive status measured by the MMSE and the MDRS were within the normal range for all participants (Table 1). A neurologic examination, performed by a blinded movement disorder specialist, excluded all signs of possible or probable FXTAS.

3.1. Gray matter voxel-based morphometry

When contrasting the gray matter volume between groups, the clusters surviving FWE correction and showing a lower gray matter volume in premutation carriers were located in the anterior lobule VI of the cerebellum (center of gravity of the clusters in the MNI space −39, −45, −28.5 and 39, −42, −29) and in the thalamus (3, −6, 9) bilaterally (Fig. 1). The term center of gravity refers throughout the article to the voxel with maximum t value or local maxima. The progression of gray matter atrophy with age in these regions is similar in the premutation and control group and there are no interactions with age, CGG, age × CGG between the 2 groups. Trends are described in Supplementary Table S1. No regions showed any increase in gray matter volume in the carrier group.

3.2. White matter: radial and mean diffusivity

Group analysis showed increased RD values in carriers in only 4 clusters including the MCPs (20, −31, −33 and −15, −28, −33) and the hippocampal fimbria/fornix and stria terminalis bilaterally (prominent band of white matter along the superomedial edge of the hippocampus; −33, −25.5, −7.5 and 28.5, −27, −4.5, respectively). These regions are significant at $p = 0.005$ uncorrected and survive small volume correction (see Section 2). Their symmetry and known association with FXTAS support the validity of the findings (Greco et al., 2006; Sevin et al., 2009; Wang et al., 2012) (Fig. 2, Supplementary Fig. S1). The mean diffusivity maps show the same alterations (Supplementary Fig. S2). Interaction (age × group)

Table 1
Descriptive statistics of the participants

Parameter	Premutation (n = 27)			Control (n = 35)			p value
	Mean	SD	Range	Mean	SD	Range	
Age (y)	46.7	12.5	20–70	42.9	11.8	20–66	ns
FMR1 CGG repeat size	85.4	26.3	57–156	31.8	6.7	20–54	<0.001
Educational level	2.2	0.8	1–3	2.4	0.7	1–3	ns
MDRS global score	140.3	3	133–144	141.6	2.7	130–144	ns
MMSE score	28.4	1	26–30	28.9	1.1	26–30	ns

Key: MDRS, Mattis Dementia Rating Scale; MMSE, Mini Mental State Examination.

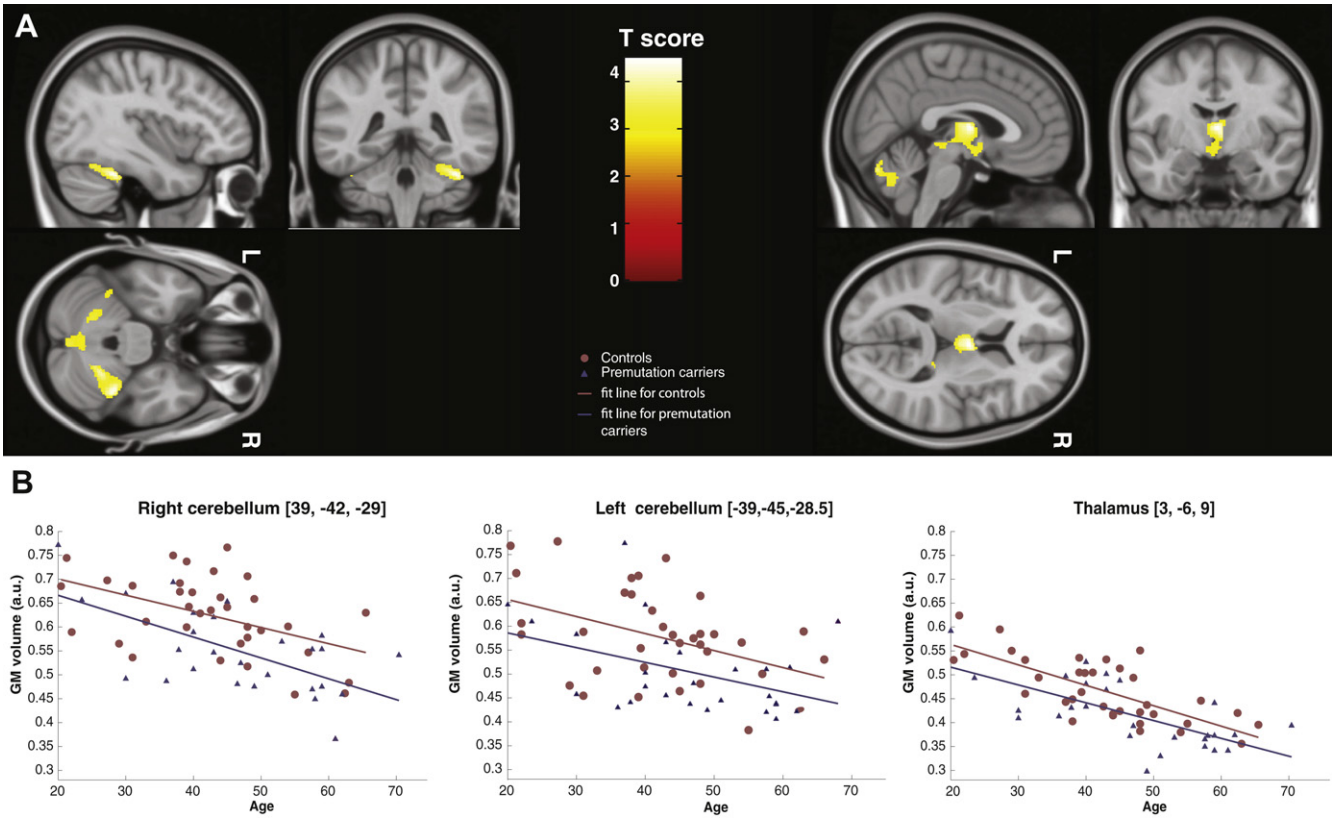

Fig. 1. Voxel-based morphometry results on gray matter. The statistical parametric maps (A) show bilateral clusters in the cerebellum (lobule VI, anteriorly) and in the thalamus where gray matter volume is lower in premutation carriers compared with controls. Maps are thresholded at $p < 0.005$ and $k > 40$ and superposed on a standard brain in the MNI (Montreal Neurological Institute) space. Hot color bar represents T scores. (B) Correlation between the modulated gray matter intensity at the center of gravity of the significant clusters and age. Effect of age in gray matter volume is similar in the premutation group compared with controls. Lines represent the fitting of the distribution of the values for the 2 cohorts.

analysis shows significant ($p < 0.05$, FWE corrected) accelerated alteration of MD and RD values with age in the premutation group in 3 large clusters centered in the frontal white matter area (42, 32, 9), and in the corticospinal tracts (centers in the posterior and superior corona radiata; −27, −28, 31 and 21, −21, 43, respectively). The latter clusters extend posteriorly into the parietal region (intraparietal sulci; −19.5, −51, 45) (Fig. 3) with a slight predominance in the left hemisphere. These regions seemed to reflect a more diffuse white matter involvement. The same region also showed interaction with CGG repeats. The MCPs showed interaction with age, length of CGG repeats, and age × CGG. Trends observed for additional clusters identified in the interaction analysis, and visible in Fig. 3, are presented in Supplementary Table S2.

3.3. White matter: fractional anisotropy and axial diffusivity

These 2 maps identified the same aforementioned clusters, both in the group (decrease of FA and increase of axial diffusivity in carriers compared with controls) and interaction analyses, but the levels of significance were lower overall. These trends are described in Supplementary Table S3.

3.4. MTR results

Among the 2 regions identified by increased MD and RD values, the MCPs are characterized by a significant decrease in mean MTR in carriers ($p = 0.05$ for both right and left MCP). The diffuse cerebral white matter region identified through interaction analyses also shows different distribution of MTR values between the 2 cohorts (Kolmogorov-Smirnov; $p < 0.001$) (Supplementary Fig. S3).

3.5. Correlation with FXTAS score

The total score of the FXTAS rating scale is within the normal range in carriers and multiple linear regression accounting for age did not find a correlation between this score and any of the aforementioned regions identified through group effects or interactions. However, the MD values in the anterior cingulate cortex correlate negatively with the FXTAS score (Supplementary Fig. S4).

4. Discussion

Our study demonstrates unique anatomic patterns of preclinical changes in young asymptomatic premutation carriers using a multimodal imaging approach to characterize brain tissue properties. We show that among lesions previously characterized in patients with FXTAS (Brunberg et al., 2002; Hashimoto et al., 2011a; Hashimoto et al., 2011b; Wang et al., 2012), cerebellar and hippocampal alterations are present in asymptomatic carriers (mean age 47 years). We interpret the presence of decreased gray matter volume with normal rates of age-related atrophy (no age × group interaction) in the cerebellum and thalamus as early alterations. The white matter changes in the hippocampal fimbria are consistent with the same interpretation. In contrast, the diffuse cerebral hemispheric white matter changes identified through an

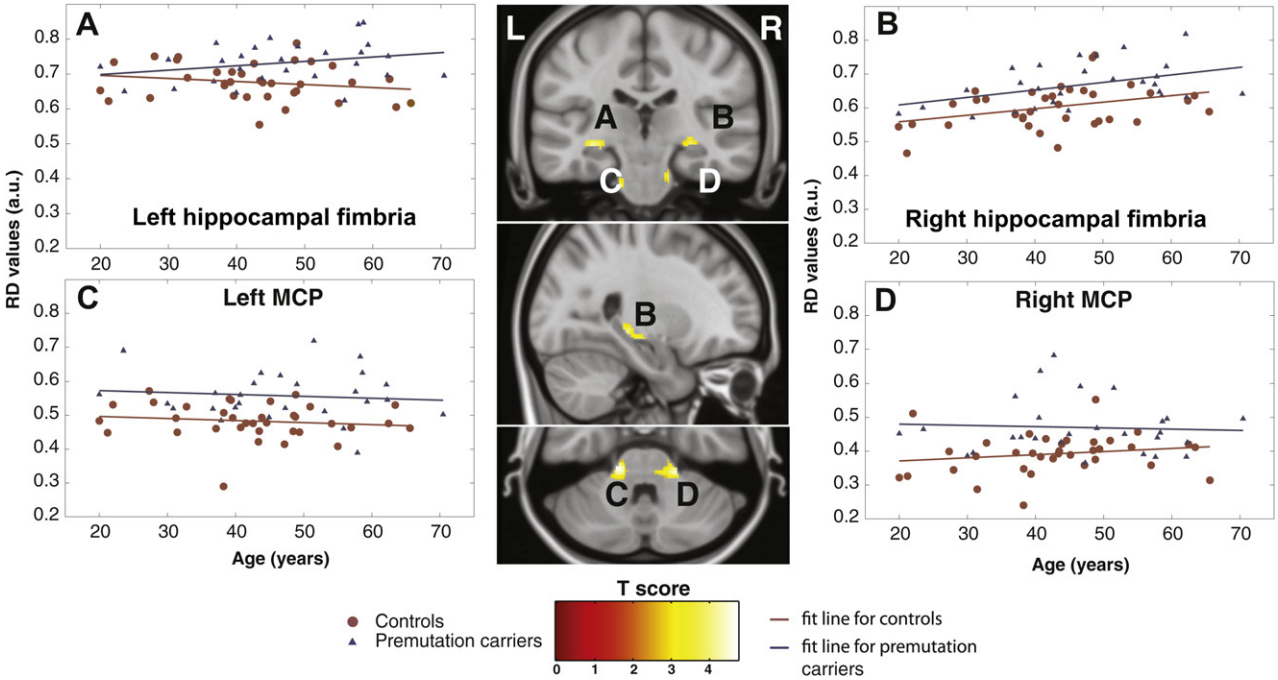

Fig. 2. Voxel-based analysis using the radial diffusivity (RD) map, showing tissue property alterations of white matter in premutation carriers. Statistical parametric map shows clusters where RD values are higher in premutation carriers compared with controls. These are located bilaterally in the middle cerebellar peduncles and in the fimbria/fornix. Letters A, B, C and D label the clusters in the coronal, sagittal, and axial (top to bottom) sections. Maps are thresholded at $p < 0.005$ and $k > 40$ and superposed on a standard brain in the MNI (Montreal Neurologic Institute) space. Hot color bar represents T scores. The 4 graphs show the correlation between the RD values at the center of gravity of each cluster and age. Lines represent the fitting of the distribution of the values for the 2 cohorts.

age × group interaction are interpreted as late stage lesions, which may mark the imminent onset of FXTAS.

The whole-brain voxel-based analysis identified alterations in the cerebellar motor network in presymptomatic carriers compared with controls (Figs. 1 and 2). The MCP and the corresponding cerebellar gray matter (anterior part of lobule VI) receiving these cortical projections are altered early on, suggesting that there may be a direct causal relationship between these 2 alterations. Neuropathologic studies have hypothesized that Purkinje cell dropout in patients with FXTAS is secondary to MCP white matter lesions (Greco et al., 2006).

However, the decrease in cerebellar gray matter volume is the most significant finding in these asymptomatic carriers and is compatible with the opposite hypothesis. Gray matter reduction in the anterior cerebellum is among the most salient findings in patients with FXTAS (Hashimoto et al., 2011a). Damage to the anterior lobe (including lobule VI) has also been correlated with ataxia scales (International Cooperative Ataxia Rating Scale) in VBM studies of patients with cerebellar lesions (Schoch et al., 2006).

Late-onset diffuse hemispheric white matter alterations are not specific, but are systematically present on FLAIR images in patients with severe forms of FXTAS (Brunberg et al., 2002). Although our findings do not show a group effect, accelerated age-related changes in diffuse cerebral white matter clusters (MD and RD values revealed by age × group interaction analysis), suggest that these lesions (as opposed to those in the MCP) appear later and much closer to the mean age of onset of FXTAS (Fig. 3). These changes, therefore, may potentially serve as markers of an imminent onset of clinical symptoms. Associated diffuse cerebral gray matter atrophy has been previously demonstrated in patients with FXTAS (Hashimoto et al., 2011a), but it was not detected in our premutation group, suggesting that it may manifest later and be secondary to white matter disease.

Changes in tissue structure seen before the onset of a neurodegenerative disorder are considered to represent a slow degenerative process (Paulsen et al., 2010). This view is being challenged and recent studies have shown that neurodevelopmental changes may be involved in adult late-onset neurodegenerative disorders, such as Huntington disease (Nopoulos et al., 2011). In our premutation group, a decrease in gray matter density in the cerebellum and thalamus is present decades before the onset of FXTAS and does not show accelerated decline with age, which one would expect in a neurodegenerative disease (Fig. 2 and Supplementary Table S1). Although it is unknown if the decrease in thalamus volume has a direct role in the onset of FXTAS symptoms, cerebellar lesions are clearly implicated in this movement disorder. This suggests that certain brain lesions classically observed in FXTAS may be the result of neurodevelopmental processes. This is consistent with findings of a recent study showing impaired embryonic neocortical development in mice expressing premutation alleles (Cunningham et al., 2011).

We show that changes in the hippocampal fimbria/fornix and the stria terminalis, a region altered in patients with FXTAS (Wang et al., 2012), are present early on. Hippocampal neurons have one of the highest rates of intranuclear inclusion density in patients with FXTAS (Greco et al., 2002; Greco et al., 2006), and developmental abnormalities were also demonstrated in murin hippocampal neurons of mice expressing a premutation allele (Chen et al., 2010).

The MTR and DTI-derived quantitative maps are sensitive to different tissue property changes in the white matter. In the MCP, an increase in MD and RD and a decrease in MTR support a myelin-based phenomenon. This pattern was observed in the hemispheric white matter, where differences in the distribution of MTR values also support myelin-related alterations (Supplementary Fig. S3). In contrast to the MCPs, the complex architecture of the hippocampus precludes any interpretation of the MD and RD values as

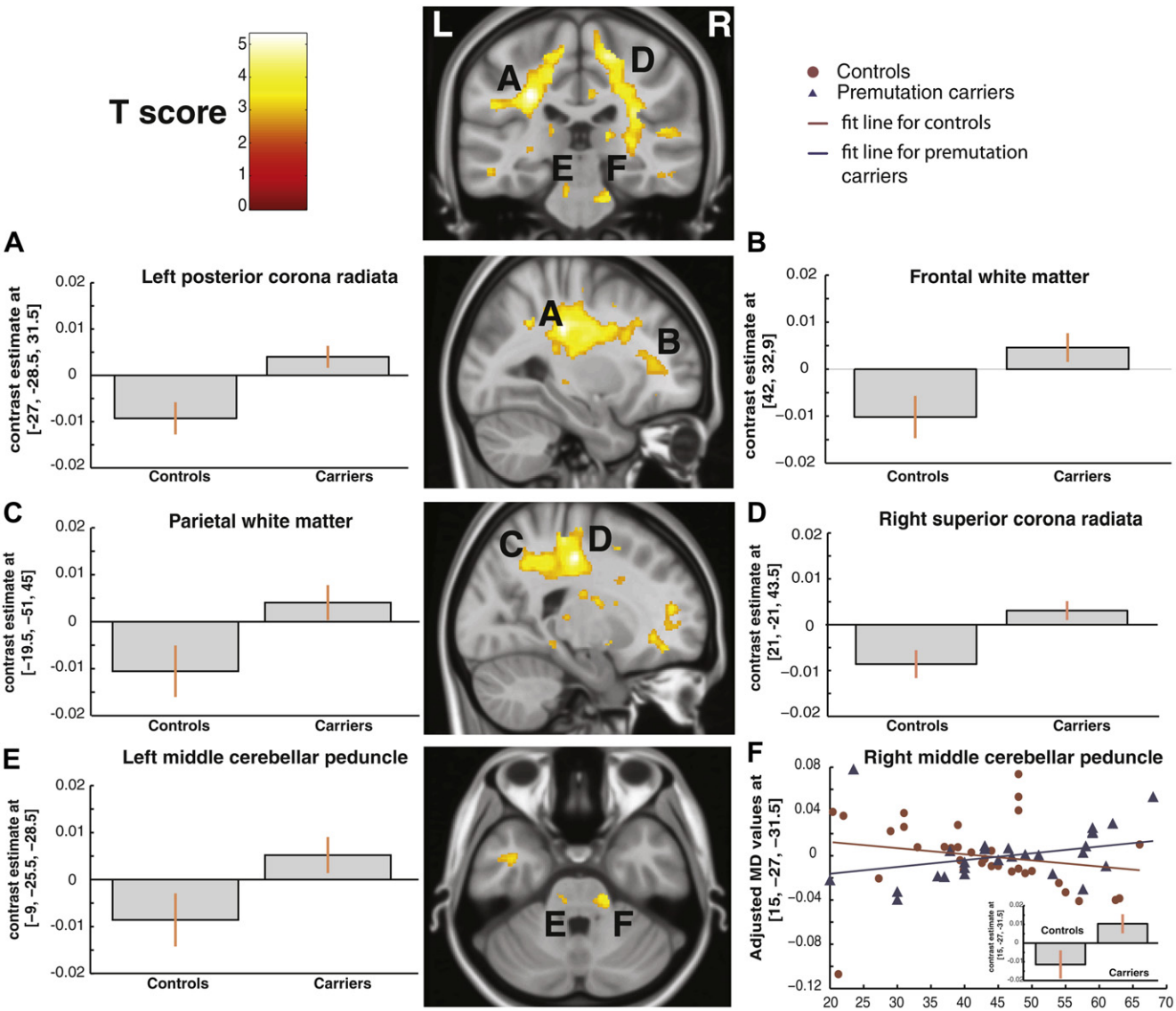

Fig. 3. Voxel-based analysis on diffusion parameters (mean diffusivity [MD]); age × group interaction analysis. Statistical parametric maps show clusters where the MD values progress with age faster in carriers compared with controls. Letters label the center of gravity of the regions located in the left posterior corona radiata (A), frontal white matter (B), parietal white matter (C), right superior corona radiata (D), and in the middle cerebellar peduncles (E and F). The diffuse white matter involvement in the cerebral hemispheres is not associated with a group effect, suggesting a late-onset mechanism. Maps are thresholded at $p < 0.005$ and $k > 40$ and superposed on a standard brain in the MNI (Montreal Neurologic Institute) space. Hot color bar represents T scores. The histograms show the beta values of the age × group interaction for the 2 groups. The scatter plot represents the adjusted MD values for the contrast of interest (interaction age × group) in the model with respect to age. To avoid redundancy, we included in the figure 1 example corresponding to the right middle cerebellar peduncle.

myelin-related alterations (Wheeler-Kingshott and Cercignani, 2009). The trends on the FA map reflect the MD and RD results and suggests that axonal loss may be secondary to myelin sheet alterations.

Accurate markers are required for the development of future neuroprotective treatments. An ideal imaging biomarker should correlate with disease progression and be present many years before the onset of the disorder (Weir et al., 2011). Although we identified early markers, our study was not designed to evaluate disease progression (only asymptomatic carriers were included). Keeping in mind the constraints due to limited variance in the FXTAS score of our premutation group, we observed a correlation between this score and the anterior cingulate cortex. Decrease in gray matter volume of the latter region has previously been reported in patients with FXTAS (Hashimoto et al., 2011a). Longitudinal studies are required to assess the relationship between these markers and disease progression.

In conclusion, alterations of the cerebellar network, present decades before the onset of FXTAS, and later diffuse involvement of the hemispheric white matter may serve as markers of distinct stages (early vs. imminent onset) of this disorder. Other changes may reflect a potential neurodevelopmental effect of the premutation. Although data in the hemispheric region supports demyelination as a primary mechanism, the robust decrease of cerebellar gray matter may favor a process in which neuronal depletion is the *primum movens*.

Disclosure statement

The authors declare no conflicts of interest.

Acknowledgements

The authors are indebted to all the families and individuals who participated in this study. Special thanks to the UK Fragile X Society and the Association Nationale du Syndrome de l'X Fragile, le Goéland for their precious collaboration. The study was supported by the Swiss National Fund 320030_122674, Centre d'Imagerie Bio-Médicale (CIBM) of the University of Lausanne (UNIL), the Swiss Federal Institute of Technology Lausanne (EPFL), the University of Geneva (UniGe), the Centre Hospitalier Universitaire Vaudois (CHUV), the Hôpitaux Universitaires de Genève (HUG), and the Leenaards and the Jeantet Foundations. The authors acknowledge Marina Grasso for her contribution in the recruitment of the participants and for the DNA testing. The authors also acknowledge Professor Gunnar Krueger for his support with setting up the MR sequences, and Dr C. Wider for his input in the manuscript editing. This work was supported by the Swiss National Fund 320030_122674 and the Synapsis Foundation, Switzerland. PH was supported by the Leenaards Foundation. SJ was supported by a grant from the Faculté de Biologie et de Médecine, Relève Académique.

Appendix A. Supplementary data/material

Supplementary data associated with this article can be found, in the online version, at http://dx.doi.org/10.1016/j.neurobiolaging.2012.12.001.

References

Anik, Y., Iseri, P., Demirci, A., Komsuoglu, S., Inan, N., 2007. Magnetization transfer ratio in early period of Parkinson disease. Acad. Radiol. 14, 189–192. http://dx.doi.org/10.1016/j.acra.2006.11.005.

Ashburner, J., 2007. A fast diffeomorphic image registration algorithm. Neuroimage 38, 95–113. http://dx.doi.org/10.1016/j.neuroimage.2007.07.007.

Ashburner, J., Friston, K.J., 2005. Unified segmentation. Neuroimage 26, 839–851. http://dx.doi.org/10.1016/j.neuroimage.2005.02.018.

Bourgeois, J.A., Seritan, A.L., Casillas, E.M., Hessl, D., Schneider, A., Yang, Y., Kaur, I., Cogswell, J.B., Nguyen, D.V., Hagerman, R.J., 2011. Lifetime prevalence of mood and anxiety disorders in fragile X premutation carriers. J. Clin. Psychiatry 72, 175–182. http://dx.doi.org/10.4088/JCP.09m05407blu.

Brouwer, J.R., Huizer, K., Severijnen, L.A., Hukema, R.K., Berman, R.F., Oostra, B.A., Willemsen, R., 2008. CGG-repeat length and neuropathological and molecular correlates in a mouse model for fragile X-associated tremor/ataxia syndrome. J. Neurochem. 107, 1671–1682. http://dx.doi.org/10.1111/j.1471-4159.2008.05747.x.

Brunberg, J.A., Jacquemont, S., Hagerman, R.J., Berry-Kravis, E.M., Grigsby, J., Leehey, M.A., Tassone, F., Brown, W.T., Greco, C.M., Hagerman, P.J., 2002. Fragile X premutation carriers: characteristic MR imaging findings of adult male patients with progressive cerebellar and cognitive dysfunction. AJNR Am. J. Neuroradiol. 23, 1757–1766.

Chen, Y., Tassone, F., Berman, R.F., Hagerman, P.J., Hagerman, R.J., Willemsen, R., Pessah, I.N., 2010. Murine hippocampal neurons expressing Fmr1 gene premutations show early developmental deficits and late degeneration. Hum. Mol. Genet. 19, 196–208. http://dx.doi.org/10.1093/hmg/ddp479.

Cornish, K.M., Kogan, C.S., Li, L., Turk, J., Jacquemont, S., Hagerman, R.J., 2009. Lifespan changes in working memory in fragile X premutation males. Brain Cogn. 69, 551–558. http://dx.doi.org/10.1016/j.bandc.2008.11.006.

Crum, R.M., Anthony, J.C., Bassett, S.S., Folstein, M.F., 1993. Population-based norms for the Mini-Mental State Examination by age and educational level. JAMA 269, 2386–2391.

Cunningham, C.L., Martinez Cerdeno, V., Navarro Porras, E., Prakash, A.N., Angelastro, J.M., Willemsen, R., Hagerman, P.J., Pessah, I.N., Berman, R.F., Noctor, S.C., 2011. Premutation CGG-repeat expansion of the Fmr1 gene impairs mouse neocortical development. Hum. Mol. Genet. 20, 64–79. http://dx.doi.org/10.1093/hmg/ddq432.

Dousset, V., Grossman, R.I., Ramer, K.N., Schnall, M.D., Young, L.H., Gonzalez-Scarano, F., Lavi, E., Cohen, J.A., 1992. Experimental allergic encephalomyelitis and multiple sclerosis: lesion characterization with magnetization transfer imaging. Radiology 182, 483–491.

Draganski, B., Ashburner, J., Hutton, C., Kherif, F., Frackowiak, R.S., Helms, G., Weiskopf, N., 2011. Regional specificity of MRI contrast parameter changes in normal ageing revealed by voxel-based quantification (VBQ). Neuroimage 55, 1423–1434. http://dx.doi.org/10.1016/j.neuroimage.2011.01.052.

Dumas, E.M., van den Bogaard, S.J., Ruber, M.E., Reilman, R.R., Stout, J.C., Craufurd, D., Hicks, S.L., Kennard, C., Tabrizi, S.J., van Buchem, M.A., van der Grond, J., Roos, R.A., 2012. Early changes in white matter pathways of the sensorimotor cortex in premanifest Huntington's disease. Hum. Brain Mapp. 33, 203–212. http://dx.doi.org/10.1002/hbm.21205.

Fahn, S.T., Tolosa, E., Marin, C., 1993. Clinical rating scale for tremor. In: Jankovic, J., Tolosa, E. (Eds.), Parkinson's Disease and Movement Disorders. Williams & Wilkins, Baltimore, pp. 271–280.

Fornari, E., Knyazeva, M.G., Meuli, R., Maeder, P., 2007. Myelination shapes functional activity in the developing brain. Neuroimage 38, 511–518. http://dx.doi.org/10.1016/j.neuroimage.2007.07.010.

Fornari, E., Maeder, P., Meuli, R., Ghika, J., Knyazeva, M.G., 2012. Demyelination of superficial white matter in early Alzheimer's disease: a magnetization transfer imaging study. Neurobiol. Aging 33. http://dx.doi.org/10.1016/j.neurobiolaging.2010.11.014. 428 e7–19.

Friston, K.J., Tononi, G., Reeke Jr., G.N., Sporns, O., Edelman, G.M., 1994. Value-dependent selection in the brain: simulation in a synthetic neural model. Neuroscience 59, 229–243.

Giulietti, G., Bozzali, M., Figura, V., Spano, B., Perri, R., Marra, C., Lacidogna, G., Giubilei, F., Caltagirone, C., Cercignani, M., 2012. Quantitative magnetization transfer provides information complementary to grey matter atrophy in Alzheimer's disease brains. Neuroimage 59, 1114–1122. http://dx.doi.org/10.1016/j.neuroimage.2011.09.043.

Greco, C.M., Berman, R.F., Martin, R.M., Tassone, F., Schwartz, P.H., Chang, A., Trapp, B.D., Iwahashi, C., Brunberg, J., Grigsby, J., Hessl, D., Becker, E.J., Papazian, J., Leehey, M.A., Hagerman, R.J., Hagerman, P.J., 2006. Neuropathology of fragile X-associated tremor/ataxia syndrome (FXTAS). Brain 129 (Pt 1), 243–255. http://dx.doi.org/10.1093/brain/awh683.

Greco, C.M., Hagerman, R.J., Tassone, F., Chudley, A.E., Del Bigio, M.R., Jacquemont, S., Leehey, M., Hagerman, P.J., 2002. Neuronal intranuclear inclusions in a new cerebellar tremor/ataxia syndrome among fragile X carriers. Brain 125 (Pt 8), 1760–1771.

Habas, C., 2004. [Basic principles of diffusion tensor MR tractography]. J. Radiol. 85, 281–286.

Hagmann, P., Cammoun, L., Gigandet, X., Meuli, R., Honey, C.J., Wedeen, V.J., Sporns, O., 2008. Mapping the structural core of human cerebral cortex. PLoS Biol. 6, e159. http://dx.doi.org/10.1371/journal.pbio.0060159.

Hashimoto, R., Javan, A.K., Tassone, F., Hagerman, R.J., Rivera, S.M., 2011a. A voxel-based morphometry study of grey matter loss in fragile X-associated tremor/ataxia syndrome. Brain 134 (Pt 3), 863–878. http://dx.doi.org/10.1093/brain/awq368.

Hashimoto, R., Srivastava, S., Tassone, F., Hagerman, R.J., Rivera, S.M., 2011b. Diffusion tensor imaging in male premutation carriers of the fragile X mental retardation gene. Mov. Disord. 26, 1329–1336. http://dx.doi.org/10.1002/mds.23646.

Hessl, D., Tassone, F., Loesch, D.Z., Berry-Kravis, E., Leehey, M.A., Gane, L.W., Barbato, I., Rice, C., Gould, E., Hall, D.A., Grigsby, J., Wegelin, J.A., Harris, S., Lewin, F., Weinberg, D., Hagerman, P.J., Hagerman, R.J., 2005. Abnormal elevation of FMR1 mRNA is associated with psychological symptoms in individuals with the fragile X premutation. Am. J. Med. Genet. B Neuropsychiatr. Genet. 139B, 115–121. http://dx.doi.org/10.1002/ajmg.b.30241.

Jacquemont, S., Hagerman, R.J., Leehey, M., Grigsby, J., Zhang, L., Brunberg, J.A., Greco, C., Des Portes, V., Jardini, T., Levine, R., Berry-Kravis, E., Brown, W.T., Schaeffer, S., Kissel, J., Tassone, F., Hagerman, P.J., 2003. Fragile X premutation tremor/ataxia syndrome: molecular, clinical, and neuroimaging correlates. Am. J. Hum. Genet. 72, 869–878. http://dx.doi.org/10.1086/374321.

Jacquemont, S., Hagerman, R.J., Leehey, M.A., Hall, D.A., Levine, R.A., Brunberg, J.A., Zhang, L., Jardini, T., Gane, L.W., Harris, S.W., Herman, K., Grigsby, J., Greco, C.M., Berry-Kravis, E., Tassone, F., Hagerman, P.J., 2004. Penetrance of the fragile X-associated tremor/ataxia syndrome in a premutation carrier population. JAMA 291, 460–469. http://dx.doi.org/10.1001/jama.291.4.460 291/4/460.

Kloppel, S., Draganski, B., Golding, C.V., Chu, C., Nagy, Z., Cook, P.A., Hicks, S.L., Kennard, C., Alexander, D.C., Parker, G.J., Tabrizi, S.J., Frackowiak, R.S., 2008. White matter connections reflect changes in voluntary-guided saccades in pre-symptomatic Huntington's disease. Brain 131 (Pt 1), 196–204. http://dx.doi.org/10.1093/brain/awm275.

Leehey, M.A., Berry-Kravis, E., Goetz, C.G., Zhang, L., Hall, D.A., Li, L., Rice, C.D., Lara, R., Cogswell, J., Reynolds, A., Gane, L., Jacquemont, S., Tassone, F., Grigsby, J., Hagerman, R.J., Hagerman, P.J., 2008. FMR1 CGG repeat length predicts motor dysfunction in premutation carriers. Neurology 70 (16 Pt 2), 1397–1402. http://dx.doi.org/10.1212/01.wnl.0000281692.98200.f5.

Li, Y., Jin, P., 2012. RNA-mediated neurodegeneration in fragile X-associated tremor / ataxia syndrome. Brain Res. 1462, 112–117. http://dx.doi.org/10.1016/j.brainres.2012.02.057.

Maes, F., Collignon, A., Vandermeulen, D., Marchal, G., Suetens, P., 1997. Multimodality image registration by maximization of mutual information. IEEE Trans. Med. Imaging 16, 187–198. http://dx.doi.org/10.1109/42.563664.

Mattis, S., 1976. Mental Status Examination for Organic Mental Syndrome in the Elderly Patient. Grune and Stratton, New York.

Moll, N.M., Rietsch, A.M., Thomas, S., Ransohoff, A.J., Lee, J.C., Fox, R., Chang, A., Ransohoff, R.M., Fisher, E., 2011. Multiple sclerosis normal-appearing white matter: pathology-imaging correlations. Ann. Neurol. 70, 764–773. http://dx.doi.org/10.1002/ana.22521.

Mori, S., Zhang, J., 2006. Principles of diffusion tensor imaging and its applications to basic neuroscience research. Neuron 51, 527–539. http://dx.doi.org/10.1016/j.neuron.2006.08.012.

Nopoulos, P.C., Aylward, E.H., Ross, C.A., Mills, J.A., Langbehn, D.R., Johnson, H.J., Magnotta, V.A., Pierson, R.K., Beglinger, L.J., Nance, M.A., Barker, R.A., Paulsen, J.S., 2011. Smaller intracranial volume in prodromal Huntington's disease: evidence for abnormal neurodevelopment. Brain 134 (Pt 1), 137–142. http://dx.doi.org/10.1093/brain/awq280.

Paulsen, J.S., Nopoulos, P.C., Aylward, E., Ross, C.A., Johnson, H., Magnotta, V.A., Juhl, A., Pierson, R.K., Mills, J., Langbehn, D., Nance, M., 2010. Striatal and white matter predictors of estimated diagnosis for Huntington disease. Brain Res. Bull. 82, 201–207. http://dx.doi.org/10.1016/j.brainresbull.2010.04.003.

Pierpaoli, C., Basser, P.J., 1996. Toward a quantitative assessment of diffusion anisotropy. Magn. Reson. Med. 36, 893–906.

Schoch, B., Konczak, J., Dimitrova, A., Gizewski, E.R., Wieland, R., Timmann, D., 2006. Impact of surgery and adjuvant therapy on balance function in children and adolescents with cerebellar tumors. Neuropediatrics 37, 350–358. http://dx.doi.org/10.1055/s-2007-964904.

Sevin, M., Kutalik, Z., Bergman, S., Vercelletto, M., Renou, P., Lamy, E., Vingerhoets, F.J., Di Virgilio, G., Boisseau, P., Bezieau, S., Pasquier, L., Rival, J.M., Beckmann, J.S., Damier, P., Jacquemont, S., 2009. Penetrance of marked cognitive impairment in older male carriers of the FMR1 gene premutation. J. Med. Genet. 46, 818–824. http://dx.doi.org/10.1136/jmg.2008.065953.

Stebbins, G.T., Goetz, C.G., 1998. Factor structure of the Unified Parkinson's Disease Rating Scale: Motor Examination section. Mov. Disord. 13, 633–636. http://dx.doi.org/10.1002/mds.870130404.

Trouillas, P., Takayanagi, T., Hallett, M., Currier, R.D., Subramony, S.H., Wessel, K., Bryer, A., Diener, H.C., Massaquoi, S., Gomez, C.M., Coutinho, P., Ben Hamida, M., Campanella, G., Filla, A., Schut, L., Timann, D., Honnorat, J., Nighoghossian, N., Manyam, B., 1997. International Cooperative Ataxia Rating Scale for pharmacological assessment of the cerebellar syndrome. The Ataxia Neuropharmacology Committee of the World Federation of Neurology. J. Neurol. Sci. 145, 205–211.

van Es, A.C., van der Flier, W.M., Admiraal-Behloul, F., Olofsen, H., Bollen, E.L., Middelkoop, H.A., Weverling-Rijnsburger, A.W., Westendorp, R.G., van Buchem, M.A., 2006. Magnetization transfer imaging of gray and white matter in mild cognitive impairment and Alzheimer's disease. Neurobiol Aging 27, 1757–1762. http://dx.doi.org/10.1016/j.neurobiolaging.2005.09.042.

Wang, J.Y., Hessl, D.H., Hagerman, R.J., Tassone, F., Rivera, S.M., 2012. Age-dependent structural connectivity effects in fragile x premutation. Arch. Neurol. 69, 482–489. http://dx.doi.org/10.1001/archneurol.2011.2023.

Weir, D.W., Sturrock, A., Leavitt, B.R., 2011. Development of biomarkers for Huntington's disease. Lancet. Neurol. 10, 573–590. http://dx.doi.org/10.1016/S1474-4422(11)70070-9.

Wheeler-Kingshott, C.A., Cercignani, M., 2009. About "axial" and "radial" diffusivities. Magn. Reson. Med. 61, 1255–1260. http://dx.doi.org/10.1002/mrm.21965.

Xydis, V., Astrakas, L., Zikou, A., Pantou, K., Andronikou, S., Argyropoulou, M.I., 2006. Magnetization transfer ratio in the brain of preterm subjects: age-related changes during the first 2 years of life. Eur. Radiol. 16, 215–220. http://dx.doi.org/10.1007/s00330-005-2796-8.